CrossMark

ORIGINAL PAPER

Effect of Base Oil Structure on Elastohydrodynamic Friction

Jie Zhang[1] · Andrew Tan[1] · Hugh Spikes[1]

Abstract The EHD friction properties of a wide range of base fluids have been measured and compared in mixed sliding–rolling conditions at three temperatures and two pressures. The use of tungsten carbide ball and disc specimens enabled high mean contact pressures of 1.5 and 2.0 GPa to be obtained, comparable to those present in many rolling bearings. The measurements confirm the importance of molecular structure of the base fluid in determining EHD friction. Liquids having linear-shaped molecules with flexible bonds give considerably lower friction than liquids based on molecules with bulky side groups or rings. EHD friction also increases with viscosity for liquids having similar molecular structures. Using pure ester fluids, it is shown that quite small differences in molecular structure can have considerable effects on EHD friction. The importance of temperature rise in reducing EHD friction at slide–roll ratios above about 5% has been shown. By measuring EHD friction at several temperatures and pressures as well as EHD film thickness, approximate corrections to measured EHD friction data have been made to obtain isothermal shear stress and thus EHD friction curves. These show that under the conditions tested most low molecular weight base fluids do not reach a limiting friction coefficient and thus shear stress. However, two high traction base fluids appear to reach limiting values, while three linear polymeric base fluids may also do so. Constants of best fit to a linear/logarithmic isothermal shear stress/strain rate relationship have been provided to enable reconstruction of isothermal EHD friction behaviour for most of the fluids tested.

✉ Hugh Spikes
   h.spikes@imperial.ac.uk

[1] Tribology Group, Imperial College London, London, UK

1 Introduction

Elastohydrodynamic (EHD) contacts are present in many lubricated machine components including rolling bearings, gears, cam/follower systems, and CV joints. In most of these systems it is important to achieve as low friction as possible in order to maximise machine efficiency. However, in some components, such as traction drives, a high friction is sought, while in rolling elements bearings the friction should be as low as possible consonant with avoiding bearing slip.

The friction of EHD contacts is determined by the high non-Newtonian rheological response of the thin lubricant film to the combination of high strain rate and very high pressure present within such contacts. Very early in the experimental study of EHD lubrication, it was noted that this friction was dependent on base oil type, with paraffinic mineral oils giving lower EHD friction than naphthenic ones. It is now recognised that EHD friction is determined primarily by the structure and flexibility of the individual molecules of the base fluid since these control how easily molecular layers move past one another during shear at high pressure.

Although there have been many studies of EHD friction using different base oils, these have mainly compared just a few base fluid types or have focussed on fluids designed to give high traction. This paper measures the EHD friction properties of a wide range of fluid structures in order to explore their dependence on influence molecular structure. It should be noted that in the context of elastohydrodynamic lubrication, friction is often referred to as "traction". The two terms are synonymous, and in this paper, the term friction is used throughout.

🙋 Springer

2 Previous Work

In 1960 Rounds measured the friction properties of several mineral and synthetic base oils in a thrust ball bearing rig [1]. He found that naphthenic base oils gave higher friction than paraffinic ones, while glycols gave the lowest friction. A similar difference between naphthenic and paraffinic oils was also noted by Cecil et al. [2] using a variable speed drive and later by Gunsel and co-workers, who found that solvent-treated mineral base oils gave higher friction than hydro-treated oils, while the lowest friction was given by base oils now classified as Group III and Group IV [3].

Much systematic research to relate EHD friction to molecular structure has been driven by the design of traction fluids which requires high EHD friction [4–11]. In an important study in 1970, Hammann et al. [4] demonstrated that molecules with one, and especially with two cyclohexyl rings, gave high EHD friction. This is consistent with the finding that naphthenic base oils have higher EHD friction than paraffinic ones since the former generally have higher saturated ring content.

Hentschel [5] compared the EHD friction coefficients of a wide range of cyclic structures and concluded that the shape of the molecules was important in that irregularly shaped molecules that were likely to interlock with neighbouring molecules gave higher friction than spherical or ellipsoidal ones. Muraki [6] studied both ring and branched chain structures and found that for the latter EHD friction increased with the degree of branching. He analysed friction data using a viscoelastic Eyring model and noted that the Eyring stress decreased with degree of branching and also with molecular volume. Further work to investigate how molecular structure could be tuned to give high EHD friction was carried out by Tsubouchi et al. [7–10], Chapaton et al. [11] and Zolper et al. [12]. Tsubouchi identified five molecular characteristics that favour high EHD friction, (1) high molecular stiffness, (2) large size, (3) short alkyl chain length, (4) high melting point and (5) low molecular polarity [10]. It was envisaged that at very high strain rates and high pressures, molecular slip becomes localised between neighbouring layers of molecules, and this slip is impeded if molecules cannot easily deform or rotate. High polarity leads to strong repulsive forces between molecules reducing their ability to pack close together. In 2004, Edgar and Hurley showed that quantitative structure activity relationships (QSAR) could be used to predict EHD friction from molecular structure based on friction measurements on other molecular structures [13].

Compared to research aimed at fluids with high EHD friction, there has been less systematic work looking at influence of molecular structure on EHD friction for more conventional types of base fluid. One major limitation is that most base fluids, including synthetics, are mixtures of molecules with different structures; in part for cost reasons that preclude full purification but also because mixtures have less tendency to freeze at low temperatures than pure liquids. Thus, most studies of EHD friction properties, even those which have looked at several base fluid types, have produced only very general findings and are not easily repeated since the fluids tested cannot be reproduced exactly.

Hirst and Moore studied the EHD friction properties of a range of base fluid types in a disc machine and analysed the results using the viscoelastic Eyring shear thinning model [14]. EHD friction was highest for fluids having saturated rings or multiple side chains and lowest for polyglycols. Polyglycols based on propylene glycol gave higher friction than those based on mixed ethylene–propylene glycol.

Hetchshel also compared the EHD friction properties of different polyglycols and, like Hirst and Moore, found that all gave low EHD friction but that friction was lowest for those containing the largest proportion of ethylene glycol species [15]. He attributed the low friction of these base oils to their molecules having a "thread-like" structure and thus being able to align and have minimal interaction with molecules in neighbouring layers.

Chang et al. [16] compared the shear stress properties of a range of ester base oils using an in-contact temperature rise mapping method. They found that shear stress (and thus friction) was strongly dependent on ester structure, with long, linear chain esters having low shear stress while branching increased shear stress. Pentaerythritol (PE) esters gave somewhat lower shear stress than trimethylolpropane (TMP)-based ones.

LaFountain et al. [17] measured the EHD friction properties of three base fluids, an alkylaromatic, a polyalphaolfin and a diester and also their blends. He analysed the results using the Eying shear thinning model. Friction was in the order PAO < diester < alkylated aromatic. When blends of pairs of the base fluid types were studied, it was found that in all cases the EHD friction fell below that predicted from a linear variation of friction with composition.

Most of the above studies employed disc machines or ball-on-disc tribometers and were aimed specifically at measuring EHD friction. A number of researchers have also shown the influence of base oil type on the loss torque or efficiency of actual gears and bearings [18–22]. All have noted reduced torque for esters, polyglycols (PGs) and polyalphaolefins (PAO) compared with mineral oils. There is some variation in terms of which synthetics give lowest friction, with Yoshizaki et al. [18] finding that PAO gave lower friction than PG but Höhn et al. finding

the reverse [19, 21]. This probably originates from differences between the specific PAO and PG fluids studied.

Several studies have shown a general correlation between fluids having high EHD friction and fluids having high pressure-viscosity coefficient [3, 23, 24]. This is not surprising since the main rheological models relating shear stress, τ, and strain rate, $\dot{\gamma}$, include a term describing the low shear rate viscosity at high pressure, η_p, for example, the Eyring equation

$$\tau = \tau_\mathrm{e} \sinh^{-1}\left(\frac{\eta_\mathrm{p}\dot{\gamma}}{\tau_\mathrm{e}}\right) \tag{1}$$

and the Carreau–Yasuda equation.

$$\tau = \frac{\eta_\mathrm{p}\dot{\gamma}}{\left(1 + \left(\frac{\eta_\mathrm{p}\dot{\gamma}}{\tau_\mathrm{o}}\right)^a\right)^{(1-n)/a}} \tag{2}$$

In these equations, τ_e and τ_o are stresses at which shear thinning becomes significant, while a and n are additional constants in the Carreau–Yasuda equation.

Thus shear stress and consequently EHD friction depend directly on viscosity at high pressure, which will be greatest for fluids with high pressure-viscosity coefficients. It has also been suggested, however, that a fluid with a high pressure-viscosity coefficient has a high limiting shear stress, probably because the same molecular factors such as molecular flexibility and the presence of side groups and saturated rings contribute to both [3].

It should be noted that there is also a well-known correlation between pressure-viscosity and temperature viscosity coefficient [25, 26] that can be explained in thermodynamic terms [27], so that fluids with high pressure-viscosity coefficient also have high temperature viscosity coefficient or low viscosity index (VI). This means that there is also a very general correlation, at least within a given base fluid type, between fluids having high EHD friction and fluids having low VI, and vice versa.

3 Test Methods

3.1 EHD Friction Curves

EHD friction was measured using a mini-traction machine (MTM2, PCS Instruments). In this a ball is loaded against the flat surface of a disc immersed in lubricant in a test chamber. The ball axis is inclined to eliminate spin in the contact, and both ball and disc are driven by separate motors to enable any chosen combination of surface speeds, u_1 and u_2. Friction measurements were made at a fixed load and entrainment speed over series of SRR values to obtain *traction curves*. At each value of SRR, pairs of measurements were made with positive and negative SRR (ball travelling, respectively, slower and faster than the disc), and these were combined to produce a mean value from which rolling friction was eliminated.

A tungsten carbide disc and ball were used for all measurements. The ball had diameter 12.7 mm. The high elastic modulus of tungsten carbide combined with the small ball size enabled high contact pressures to be reached at quite low loads. The disc used had a measured roughness value, R_q, of 7.0 nm, and the ball had a roughness value, R_q, of 14.4 nm, so the composite roughness was 16 nm.

Tests were carried out at three temperatures, 60, 80 and 100 °C, and two applied loads, 22.7 and 53.7 N, corresponding to mean Hertz pressures of 1.5 and 2.0 GPa, respectively.

At each load and temperature combination, the entrainment speed was held constant at 2.0 m/s, and the slide–roll ratio was increased from 0 to 50% in 24 stages. Slide–roll ratio, SRR, is defined by SRR = $|u_1 - u_2|/U$, where U is the entrainment or mean rolling speed, $U = (u_1 + u_2)/2$.

Each fluid was tested three times, and the average at each SRR was calculated.

3.2 EHD Film Thickness

The EHD film-forming properties of the test oils were also measured in order both to ensure that friction measurements were made in full film EHD conditions and also to enable calculation of the mean shear rates present in the frictional contacts.

EHD film thickness was measured using an EHD2 Ultra Thin Film Measurement System from PCS Instruments, Acton, UK. This combines a spacer layer with spectrometry to measure central EHD film thickness in a rolling or rolling–sliding reflective ball on transparent disc lubricated contact, as described in [28]. In this study, a steel ball/glass disc combination was employed, and central film thickness, h_c, was measured at three temperatures 60, 80 and 100 °C as a function of entrainment speed, U. Tests were carried out in nominally pure rolling with the disc driving the ball.

In addition to EHD film thickness, refractive index was measured in order to convert optical film thickness to spatial film thickness, while low shear rate viscosity was measured using a Stabinger SVM 3000 viscometer.

4 Test Fluids

The 38 test fluids studied are listed in Table 1. The majority of these were base oils, but PIB, MO1, MO2 and the four PAOs all contained 2.3 wt% of a mild S–P anti-wear/extreme pressure additive. However, this level of anti-wear additive should have negligible effect on the EHD friction properties of the lubricants.

Table 1 Lubricants tested

E1	Dibasic acid ester	Di(2-ethylhexyl)phthalate
E2	Dibasic acid ester	Di-*n*-octyl phthalate
E3	Dibasic acid ester	Bis(2-ethylhexyl)terephthalate
E4	Dibasic acid ester	Bis(2-ethylhexyl)adipate
E5	Dibasic acid ester	Di(2-ethylhexyl)azelate
E6	Dibasic acid ester	Bis(2-ethylhexyl)sebacate
E7	Dibasic acid ester	Diisodecylazelate
E8	Polyol ester	NPG dioleate
E9	Polyol ester	NPG diisostearate
E10	Polyol ester	TMP C8/C10
PG1	Polyalkylene glycol	TMP 3:1 EO:PO
PG2	Polyalkylene glycol	Glycerol 1:1 EO:PO
PG3	Polyalkylene glycol	Butanol propoxylate (22cSt)
PG4	Polyalkylene glycol	Butanol propoxylate (30cSt)
PG5	Polyalkylene glycol	C12–C14 propoxylate
PG6	Polyalkylene glycol	PPG-10 cetyl ether
PG7	Polyalkylene glycol	PPG-3 myristyl ether
PAO1	Polyalphaolefin	PAO (1.7 cSt at 100 °C)
PAO2	Polyalphaolefin	PAO (5.5 cSt at 100 °C)
PAO3	Polyalphaolefin	PAO (7 cSt at 100 °C)
PAO4	Polyalphaolefin	PAO (12 cSt at 100 °C)
MO1	Mineral oil	Group 1
MO2	Mineral oil	Group 2
MO3	Mineral oil	Group 3 (4 cSt at 100 °C)
MO4	Mineral oil	Group 3 (6.5 cSt at 100 °C)
MO5	Mineral oil	Group 3 (7.5 cSt at 100 °C)
TF1	Traction base fluid	2,4-Dicyclohexyl-2-methylpentane
TF2	Traction base fluid	2,3-Dimethyl-2-[(3-methylbicyclo[2.2.1] hept-2-yl)methyl]bicyclo[2.2.1]heptane
PIB	Polyisobutylene	PIB
PFPE1	Perfluoropolyether	Z25
PFPE2	Perfluoropolyether	Z09
PFPE3	Perfluoropolyether	Krytox 15–25
NO1	Natural oil	High oleic sunflower oil
NO2	Natural oil	Soybean oil
NO3	Natural oil	Castor oil
IL1	Ionic liquid	Methyltrioctylammonium bis(trifluoromethylsulfonyl)imide
IL2	Ionic liquid	1-Ethyl-3-methylimidazolium ethyl sulphate
IL3	Ionic liquid	1-Butyl-3-methylimidazolium tetrafluoroborate

Fluids E1–E4 and E6 and the three ionic liquids originated from chemical companies and can be considered to be at least 99% pure, but the other fluids, which were sourced from commercial lubricant suppliers, have unspecified purity; their name indicates the predominate species present. The structures of these fluids are described in "Appendix 1".

5 Results

5.1 Viscometics

Table 2 lists the dynamic viscosities, η, of the fluids at the three test temperatures as well as their kinematic viscosities at 40 and 100 °C and their viscosity indices.

Table 2 Viscosities of tested lubricants

Fluid	KV40 (mm^2/s)	KV100 (mm^2/s)	VI	η 60 °C (mPas)	η 80 °C (mPas)	η 100 °C (mPas)
E1	26.9	4.20	86	11.6	6.27	3.89
E2	17.9	3.67	80	8.85	5.16	3.37
E3	28.9	4.64	58	12.6	6.89	4.28
E4	7.75	2.34	121	4.21	2.84	2.03
E5	10.7	3.04	151	5.66	3.69	2.61
E6	11.5	3.18	150	6.00	3.88	2.73
E7	18.1	4.46	168	8.96	5.58	3.81
E8	27.6	6.54	205	13.3	8.2	5.54
E9	46.5	8.13	149	19.6	11.0	6.88
E10	20.1	4.51	143	9.90	5.98	3.99
PG1	968	158	280	478	262	162
PG2	137	21.6	186	64.9	35.3	21.8
PG3	128	22.3	204	58.9	33.0	20.9
PG4	175	30.2	215	80.4	44.9	28.3
PG5	133	23.5	209	45.9	26.0	21.8
PG6	29.1	6.10	165	13.7	8.14	5.33
PG7	15.9	3.66	116	7.57	4.62	3.11
PAO1	5.22	1.69	–	2.51	1.73	1.26
PAO2	28.1	5.37	120	11.5	6.63	4.17
PAO3	43.1	7.12	118	16.8	9.09	5.57
PAO4	92.0	12.0	118	32.7	16.6	9.50
MO1	32.9	5.59	108	13.2	7.34	4.59
MO2	32.1	5.53	109	12.8	7.15	4.48
MO3	19.0	4.11	118	8.4	5.11	3.21
MO4	36.8	6.38	125	14.5	8.10	5.04
MO5	47.2	7.72	131	18.2	9.97	6.12
TF1	18.77	3.49	28	7.89	4.50	2.95
TF2	22.7	4.07	57	10.33	5.85	3.77
PIB	29.7	4.8	70	11.1	6.09	3.79
PFPE1	160	50	351	180	120	84.4
PFPE2	55.2	17.6	338	61.7	41.6	29.5
PFPE3	82.6	10.7	114	64.8	32.5	18.8
NO1	40.9	8.75	201	20.0	12.1	7.51
NO2	41.2	8.90	204	20.6	12.5	7.77
NO3	254	19.5	86	82.9	36.0	17.6
IL1	208	19.7	108	84.8	38.7	25.6
IL2	39.0	7.76	174	24.1	14.1	9.21
IL3	43.9	7.76	147	25.0	14.1	8.92

5.2 EHD Film Thickness

Film thickness measurements were made for all fluids at the three test temperatures. These were then adjusted to predict the film thicknesses in the MTM friction tests by taking account of the stiffer materials (WC), smaller ball radius and differing loads in the latter using the Dowson and Chittenden EHD point contact equation [29]. This showed that all subsequent MTM friction measurements were made at a lambda ratio (ratio of central film thickness to composite surface roughness) of greater than 1.8, and in most cases greater than 2.5. Lambda ratios less than 2 occurred only for PAO1, E4 and E6 at the highest test temperature.

5.3 EHD Friction

Figure 1 shows a typical set of EHD friction curves (traction curves) for one of the test fluids. These have the typical form of a rapid increase in friction coefficient with

SRR followed by levelling out and eventually a drop at high SRR. Friction coefficient increases with contact pressure and decreases with temperature. The fall in friction coefficient at high SRR is generally accepted to result from shear heating of the EHD film due to a temperature rise of the oil film from the large quantity of frictional heat dissipated in the contact.

"Appendix 2" shows the measured friction curves for all of the fluids tested. Almost all fluids show a broadly similar pattern of behaviour, with friction increasing with pressure and decreasing with temperature. However, a few of the fluids, notably the two traction base fluids and to a lesser extent PIB and PFPE3, show EHD friction that is quite insensitive to temperature and pressure, while PFPE1 and PFPE2 show EHD friction that varies particularly strongly. The extent to which friction decreases with SRR at high SRR is quite variable, being quite small for the

esters (except for E9) and especially large for the polymeric base oils PG2–PG4 and PFPE1 and PFPE2.

Figure 2 compares the friction coefficients at 5% SRR with the maximum friction coefficients at 2 GPa mean pressure and 60 °C, the test conditions at which the friction coefficients are highest for all of the test fluids. A value of 5% SRR was chosen since this lies close to the top of the friction curve but at a sufficiently low sliding speed to limit any effect of shear heating on friction. The maximum friction coefficient value is typically 5–10% greater than the value at 5% SRR, though less so for the PFPEs and the traction fluids.

Figure 3 compares the 5% SRR friction coefficients of all the fluids at the two extremes of test condition: low temperature and high pressure, and high temperature and low pressure. Although the values at low pressure and high temperature are lower, the overall dependence of friction coefficient on base oil type remains largely unchanged.

It can be seen that the range of EHD friction coefficients is considerable, from 0.042 to 0.122 at 2.0 GPa and 60 °C. The esters, PAOs, natural oils and ionic liquids give relatively low EHD friction, while the traction fluids, PIB and the PFPEs, give high friction. The PGs are quite variable. These differences will be discussed in more detail below.

6 Discussion

6.1 Fluids with High Friction Coefficient

Fluids showing high EHD friction are the traction fluids, PIB, the PFPEs and some of the polyglycols. Previous work has highlighted the importance of molecular shape
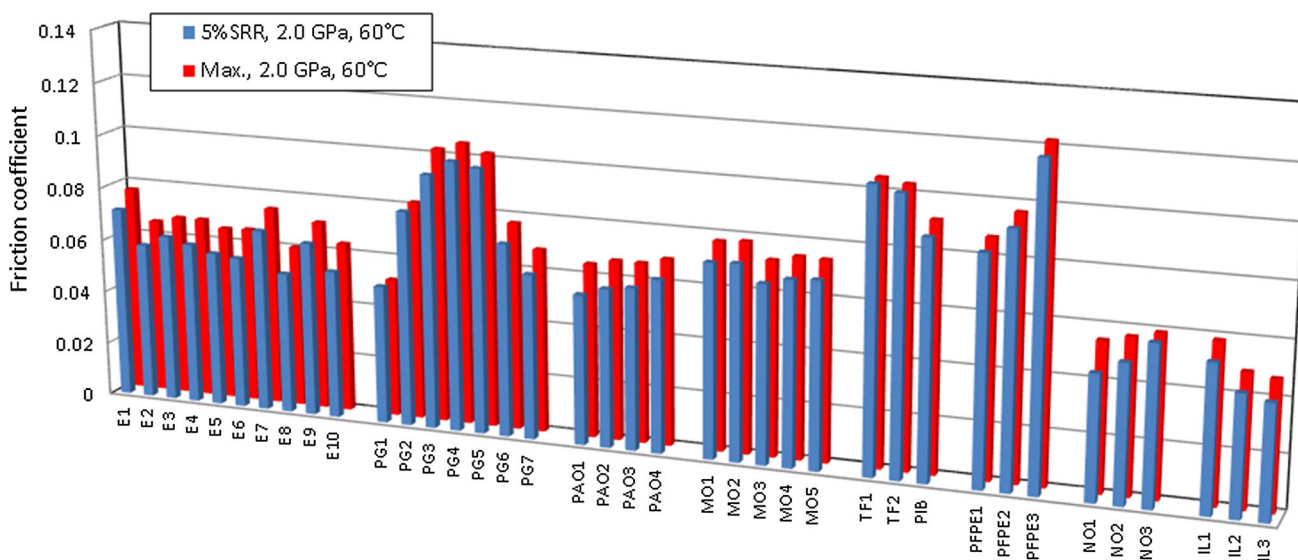

Fig. 1 EHD friction versus slide–roll ratio % for polyglycol fluid PG4 at 6 test conditions

Fig. 2 Comparison of maximum EHD friction coefficient with that measured at 5% SRR for all test fluids at mean pressure 2.0 GPa and 60 °C
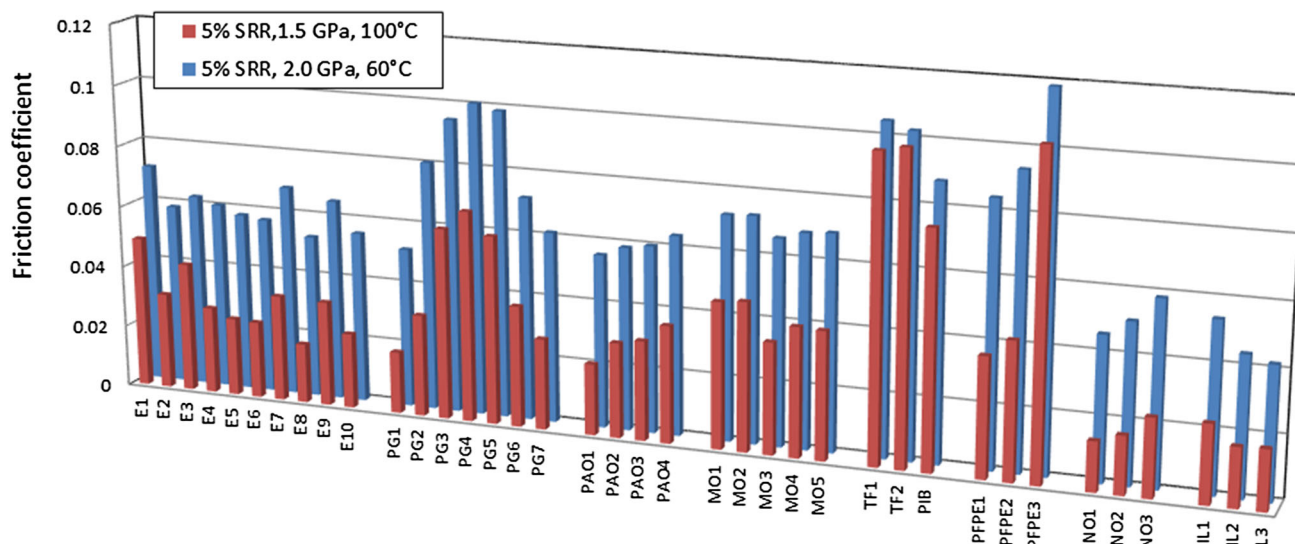
Fig. 3 Comparison of EHD friction coefficients at 5% SRR for all test fluids at two test conditions, (1) mean pressure 2 GPa and 60 °C, (2) mean pressure 1.5 GPa and 100 °C

and flexibility on EHD friction and the contribution of cyclohexyl and pendant methyl groups to high friction. Cyclohexyl rings provide bulky molecular groups that are not easily able to align or otherwise accommodate by rearrangement to high applied shear stress, while pendant CH_3 groups protrude from the molecule and hinder free sliding against neighbouring layers of molecules. Both of the traction fluid structures are based on cyclohexyl rings, while PIB has an abundance of methyl groups. It is also noteworthy that PFPE3 is the only perfluorinated polyether based on fluorinated propylene monomers and thus carrying a pendant $-CF_3$ group on each unit. These presumably contribute to this fluid's high EHD friction in a similar fashion to $-CH_3$. The other two PFPEs also show quite high EHD friction, especially at high pressure, which is quite surprising because their viscosity indices are high. It is possible that the larger and more polar fluorine atoms in the backbone provide a greater potential barrier to the passage of neighbouring molecules during interlayer slip.

The EHD friction of the PGs is determined strongly by the proportion of propylene glycol to ethylene glycol units in the molecule as noted previously by Hentschel [15]. The propylene glycol units have a pendant methyl group, while the ethylene glycol units do not. Thus PG1 has only one propylene glycol to every three ethylene glycols, PG2 has a one-to-one ratio, and PG3–PG5 contain only propylene glycols. As a consequence, the EHD friction rises progressively from PG1 to PG3. PG4 has the highest EHD friction of the polyglycols since it has a relatively small alkyl end group coupled to a long polypropylene glycol chain, so the ratio of pendant methyl groups to total molecular size is maximal. In PG5 and PG6 propylene

glycol units form only a small proportion of each molecule, so EHD friction is correspondingly lower.

6.2 Fluids with Low Friction Coefficient

Most of the synthetic esters, the natural oils, the PAOs and the ionic liquids show relatively low EHD friction. Molecular factors that promote low EHD friction are linear chains that give little interaction with neighbouring, aligned chains, flexible groups such as C–O–C and large free volume which reduces the proximity of neighbouring molecules and allows them room to adapt their conformation to applied stress. Thus, as shown in Fig. 3, PAOs, which are based on alk-1-enes and thus comprise a high proportion of linear alkyl chains, generally show lower EHD friction than mineral oils. Synthetic esters, E1–E10, that are based around the flexible C(O)–O–C linkage tend to show relatively low EHD friction, while EHD friction of natural esters NO1–NO3 is particularly low, probably due to the combination of flexible ester groups and a high degree of linearity. The pendant –OH of the ricinoleyl group in NO3 appears to increase EHD friction compared to NO1 and NO2. Biresaw and Bantchev [30] have also reported low EHD friction coefficients for natural oils. Ionic liquids show low EHD friction probably due to their having large free volume since the presence of mutually repulsive anions and cations inhibits close packing.

6.3 Friction and Molecular Structure of Esters

For the pure ester fluids, it is possible to determine some specific effects of molecular structure on EHD friction by
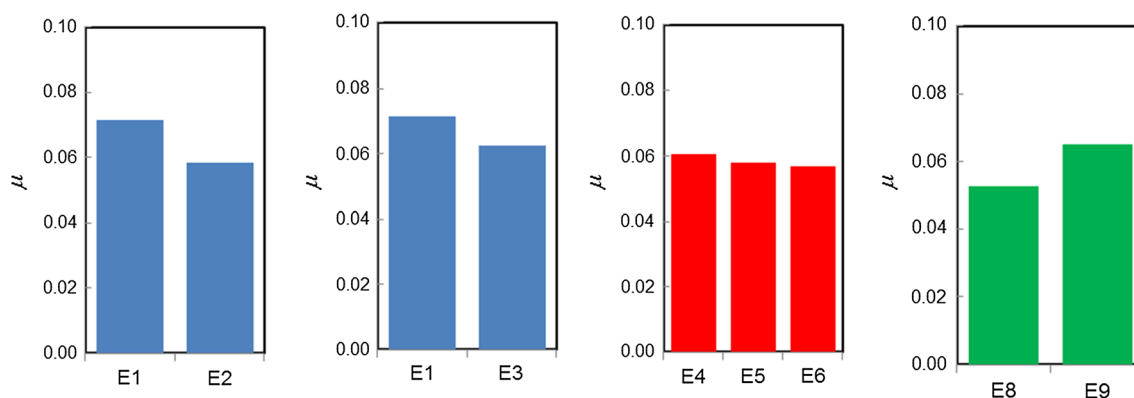
Fig. 4 Comparison of structurally related esters (5% SRR, 2 GPa, 60 °C)

comparing molecules with very similar structures. Figure 4a compares the EHD friction at 5% SRR, 2 GPa and 60 °C of the two isomers di-(2-ethylhexyl)phthalate (E1) and di-(n-octyl)phthalate (E2). The ester with linear alkyl chains gives significantly lower EHD friction than the one with branched chains. Figure 4b compares ortho- and para-isomers of a phthalate ester and shows that the para-substituent arrangement, which provides a more linear molecule, has lower EHD friction. Figure 4c compares diesters of adipic, azelaic and sebacic acid and shows that EHD friction decreases with increasing acid chain length, again illustrating the significance of molecular shape on friction. Figure 5d compares the two NPG esters E8 and E9, which are identical except that E8 is based on oleic acid and thus has a central double bond, while E9 is based on isostearic acid with no double bond but a terminal branch. E8 has considerably lower EHD friction indicating that either the double bond favours low friction or the terminal branch favours high friction or probably both. This study was constrained by the availability of structures that were

commercially available—clearly a much deeper study would be possible if ester synthesis were carried out.

6.4 Effect of Base Oil Group on EHD Friction

Figure 5 compares the EHD friction coefficients at 5% SRR of four oils from different API base fluid groups. As expected, Group 1 base oil have higher friction than Group 2, and these are usually higher than Group 3 and Group 4. This corresponds to a decreasing proportion of cyclic and branched aliphatic content.

6.5 Effect of Viscosity on EHD Friction

Within a family of very similar fluids that vary only by their mean molecular weight and thus viscosity the EHD friction coefficient increases logarithmically with low shear rate viscosity. This can be seen in Fig. 6 for the four PAOs tested at the three test temperatures where the friction coefficient at 5% SRR is plotted against low shear rate dynamic viscosity. This behaviour is expected for the same reason that EHD friction increases with pressure-viscosity coefficient as described earlier in this paper. Except at very slow slide–roll ratios, EHD friction originates almost entirely from the integral of the shear stress across the contact and most shear stress versus strain rate equations assume that shear stress increases with low shear viscosity at the prevailing contact pressure [31]. Clearly for a group of similar fluids with similar pressure-viscosity coefficients, those having the highest values of viscosity at atmospheric pressure will also tend to have the highest value at the much high pressure within the contact. Thus, at high pressure and assuming a Barus viscosity–pressure equation, the Eyring shear stress strain rate shown in Eq. 1 becomes:
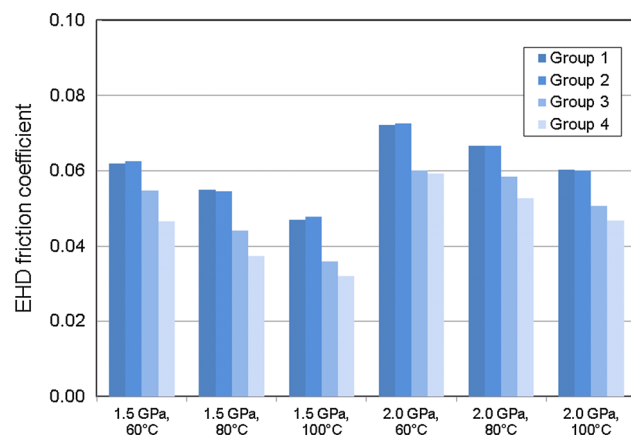

Fig. 5 Comparison of EHD friction of Group 1 (MO1), Group 2 (MO2), Group 3 (MO3) and Group 4 (PAO2) at 5% SRR

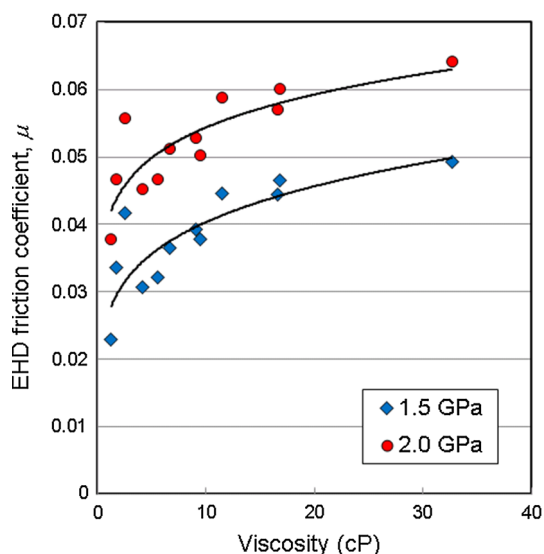$$\tau = \tau_{\mathrm{e}} \ln\left(\frac{2\eta_o e^{\alpha p}\dot{\gamma}}{\tau_{\mathrm{e}}}\right) \tag{3}$$

Fig. 6 EHD friction coefficient at 5% SRR versus low pressure viscosity for all of the PAOs at the three test temperatures

Fig. 7 Mean shear stress versus strain rate curves for polyglycol fluid PG4 at six test conditions

where η_o is the viscosity at atmospheric pressure of the lubricant and α is its pressure-viscosity coefficient. If α varies only slightly within a family of fluids, the shear stress and consequently friction increase logarithmically with η_o. In practice, α tends to increase slowly with viscosity. Even if the viscosities of the fluids do not obey the Barus equation precisely, the high pressure viscosity is still likely to vary systematically with the low pressure value within a given family of fluids.

6.6 Shear Stress Versus Strain Rate Curves

EHD friction versus slide–roll ratio plots as shown in Fig. 1 can be very easily converted to curves of mean shear stress, $\bar{\tau}$, versus strain rate, $\dot{\gamma}$. The mean shear stress is the friction force, F, divided by the area of the contact, A, and the friction force is simply the friction coefficient, μ, multiplied by the load, W. Thus the mean shear stress is the friction coefficient multiplied by the mean pressure, $\bar{p}$.

$$\bar{\tau} = \frac{F}{A} = \frac{\mu W}{A} = \mu \bar{p} \qquad (4)$$

The shear rate is the sliding speed, u_s, divided by central film thickness, h_c, while the sliding speed is the SRR multiplied by the entrainment speed, U.

$$\dot{\gamma} = \frac{u_s}{h_c} = \frac{SRR \cdot U}{h_c} \qquad (5)$$

Since W and thus $\bar{p}$, and U and thus h_c are fixed for a given EHD friction curve, from Eqs. 4 and 5, friction curves can be converted directly to a mean shear stress versus strain rate curve as long as the EHD film thickness is known.

Figure 7 shows the mean shear stress versus strain rate curves obtained by transforming the friction data for PG4 shown in Fig. 1, based on measured film thicknesses. The mean shear stress is considerably greater at 2 GPa than at 1.5 GPa.

6.7 Temperature Effect

As already noted, the shapes of EHD friction curves at high slide–roll ratios are dominated by shear heating of the EHD film that often results in a reduction in measured friction. In order to compare the intrinsic EHD friction properties of fluids and, indeed, to transfer friction measurements from one contact geometry to another, it is desirable to subtract the effect of this shear heating from the friction curves. This can be done if EHD friction is measured at several bulk temperatures. It is also of interest to determine isothermal traction curves to see whether the fluids tested reach a limiting shear stress at high strain rates or whether the levelling out and fall at high SRR seen with some fluids is due only to temperature rise.

The mean temperature rise of the oil film in the contact is the sum of the mean "flash temperature rise" of the two solid surfaces as they pass through the contact, $\Delta \bar{T}_{surf}$, and the mean temperature rise of the oil film above this surface temperature $\Delta \bar{T}_{oil}$. For a contact between surfaces of the same material, these can be calculated from an equation due to Archard [32] to give the mean oil film temperature, $\bar{T}_{oil}$ in the contact;

$$\bar{T}_{oil} = T_o + \Delta \bar{T}_{surf} + \Delta \bar{T}_{oil}$$
$$= T_o + \frac{1}{(2\pi K_s \rho c)^{0.5}} \left(\frac{2b}{U}\right)^{0.5} \dot{q}'' + \frac{h_c}{8 K_{oil}} \dot{q}'' \qquad (6)$$

where T_o is the bulk temperature, K_s, ρ and c are the thermal conductivity, density and specific heat of the surfaces, respectively, b is the contact half width and K_{oil} the

thermal conductivity of the oil film. $\dot{q}''$ is the rate of heat generation by friction per unit area of film and is given by:

$$\dot{q}'' = \frac{Fu_s}{A} = \bar{\tau} u_s = \bar{\tau} \dot{\gamma} h_c \quad (7)$$

Typical values of $\dot{q}''$ lie in the range 10^5–10^8 W/m^2. It should be noted that the constant value shown as the denominator of the second term in Eq. 6 depends on assumptions as to the velocity gradient and thus heat dissipation through the film thickness. The value 8 is derived assuming Couette shear with a rate of heat dissipation that is constant through the thickness. If the film is assumed to form a central shear plane, a value 4 is obtained [32]. If the fluid shears mainly close to the walls, as recently observed using fluorescence for polybutene [33], then, at the limit, the second term in Eq. 6 becomes negligible since heat is generated at the solid surfaces.

With the above caveat, Eqs. 6 and 7 can be used to determine the mean temperature of the oil film in the contact for each friction measurement. For tungsten carbide, the product $K_s \rho c = 3.3 \times 10^8$ J^2 K^{-2} s^{-1} m^{-4}, b was 69 μm at a load of 22.7 N and 92 μm at 53.7 N. For most lubricants, K_{oil} was estimated from data in [34] by selecting the nearest fluid type and correcting to the relevant mean contact pressures as suggested in this paper. Atmospheric pressure values for PFPEs were taken from [35] and ionic liquids from [36] and adjusted by assuming a similar conductivity–pressure dependence to other fluid types. In general, this adjustment gives thermal conductivity about 2.5 times larger at 2 GPa than at atmospheric pressure. Table 3 lists the thermal conductivities values used. Because of uncertainties in these thermal conductivities and also the denominator of the second term of the equation, it is recognised that the calculated mean temperature rises from Eq. 6 are estimates only, especially for thick EHD films since this term increases linearly with film thickness.

Table 3 Estimated thermal conductivities (W/mK)

Fluid	$p_{mean} = 1.5$ GPa	$p_{mean} = 2$ GPa
E1–E10	0.35	0.38
PG1–PG7	0.33	0.36
PAO1–PAO4	0.37	0.41
MO1–MO5, PIB	0.31	0.35
TF1, TF2	0.27	0.30
PFPE1–PFPE3	0.17	0.18
NO1–NO3	0.35	0.38
IL1	0.37	0.40
IL2	0.49	0.54
IL3	0.35	0.38

6.8 Isothermally Corrected Shear Stress and Friction Coefficient

Based on the in-contact mean oil film temperatures calculated as described in the previous section, the mean shear stresses obtained from measured friction data could be corrected back to their bulk test temperature values. For each fluid and load combination, the sets of shear stress/strain rate data points at the three temperatures were combined to form one data set, excluding values at SRRs below 1%. The resulting sets of ($\bar{\tau}$, $\dot{\gamma}$ and $\bar{T}_{oil}$) values were then fitted by a nonlinear polynomial surface of the form;

$$\bar{\tau}_{fit} = a_0 + a_1 x + a_2 x^2 + a_3 x^3 + a_4 \bar{T}_{oil} + a_5 \bar{T}_{oil}^2 + a_6 x \bar{T}_{oil} \quad (8)$$

where $x = \log_e(\dot{\gamma})$. This entirely empirical equation when best-fitted using the least squares method gave R^2 always greater than 0.96 and was able to predict all measured values to within 5% for all the test fluids.

The measured shear stresses were then adjusted to isothermal ones at the bulk test temperature using the equation:

$$\bar{\tau}_{corr(T_{bulk})} = \bar{\tau}_{meas(\bar{T}_{oil})} + \left(\bar{\tau}_{fit(T_{bulk})} - \bar{\tau}_{fit(\bar{T}_{oil})} \right) \quad (9)$$

The isothermally adjusted friction coefficients were then:

$$\mu_{corr(T_{bulk})} = \frac{\bar{\tau}_{corr(T_{bulk})}}{\bar{p}} \quad (10)$$

The precise form of Eq. 8 is not critical as long as it fits the measured data closely, especially since it is being used not to determine values of shear stress at the bulk test temperature a priori but only to correct the original shear stress measurement using the bracketed term in Eq. 9. This is generally a relatively small correction as long as only small temperature rises are considered.

Figure 8a shows the resulting, corrected, isothermal traction curves for the ten ester fluids. The curves shown are limited to a maximum of 10% SRR because the temperature calculation method based on Eq. 6 is not considered sufficiently reliable to determine temperatures rises above ca 8 °C accurately enough for shear stress correction. Figure 8b shows that the isothermally adjusted friction coefficient increases logarithmically with SRR except at the very lowest slide–roll ratio.

Figures 9, 10, 11, 12 and 13 show isothermally adjusted friction coefficient versus slide–roll ratio plots at 2 GPa and 60 °C for the Group 1–4 oils, the polyglycols, the PFPEs, the natural oils and ionic liquids and the two traction base fluids, respectively. It should be noted that Figs. 10, 11 and 13 have different ordinate scales from the other graphs, to accommodate higher EHD friction coefficients.
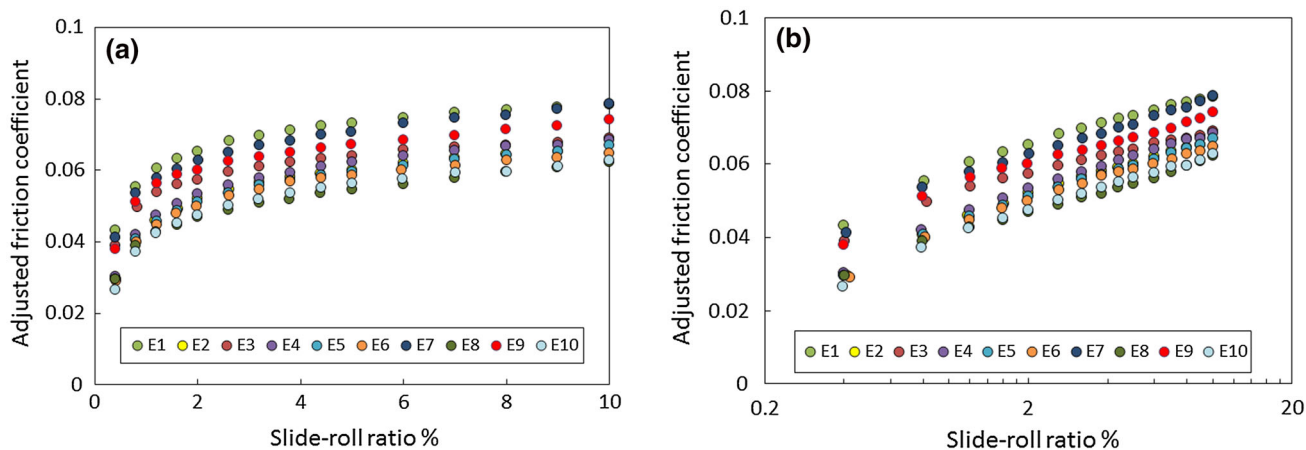
Fig. 8 Isothermally corrected EHD friction coefficient versus slide–roll ratio at mean pressure = 2 GPa, temperature = 60 °C. **a** Linear/linear plot, **b** log/linear plot
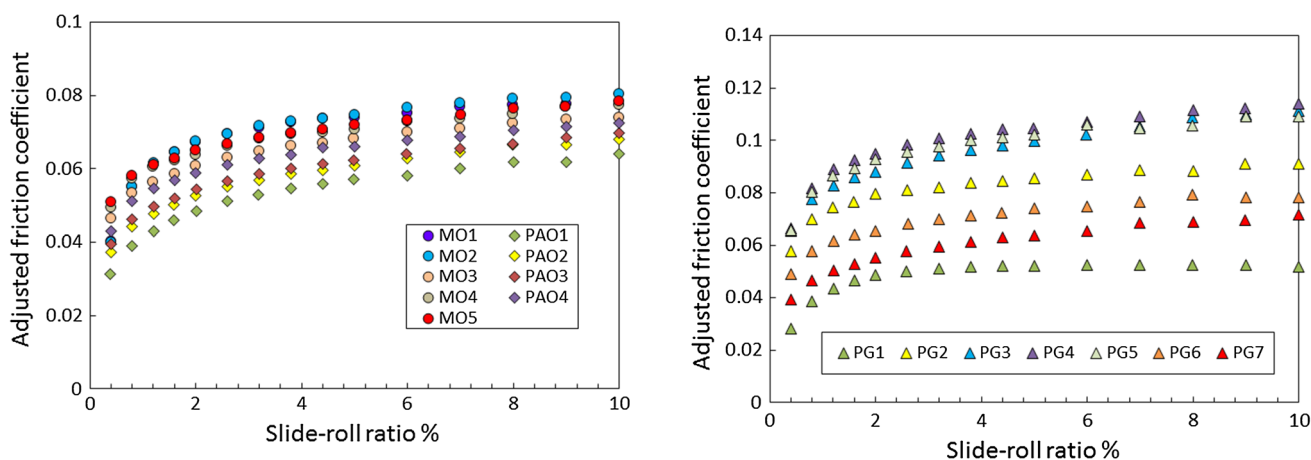

Fig. 9 Isothermally adjusted EHD friction coefficient versus slide–roll ratio for the Group 1 to 4 base oils at mean pressure = 2 GPa, temperature = 60 °C

Fig. 10 Isothermally adjusted EHD friction coefficient versus slide–roll ratio for the polyglycols at mean pressure = 2 GPa, temperature = 60 °C

Almost all fluids show friction coefficient rising linearly with log(SRR), and, for the low molecular weight fluids, such as the esters, mineral oils, PAOs, natural oils and ionic liquids, this linearity continued up to SRR = 50%, suggesting that the temperature correction was valid to 40 °C rather than the conservative 8 °C limit suggested above. The main exceptions are fluids PG1, PFPE1 and PFPE2 that continue to show a slight drop in friction at high SRR even after isothermal correction (the two PFPEs only at 1.5 GPa pressure), and the two traction fluids TF1 and TF2 that show a limiting friction coefficient. For these last two fluids, the isothermal correction has negligible effect since their EHD friction coefficients are very insensitive to temperature as well as pressure. The shape of the EHD friction curves of the two traction fluids is different at low slide–roll ratios from the other fluids. This is believed to result from a viscoelastic accommodation of strain in the entry zone of the contact in response to the very steep friction increase in this region [37].

It is interesting to note that PG1, PFPE1 and PFPE2 are structurally quite similar with long, linear molecules likely to show very little interaction between neighbouring aligned molecular layers. It is thus possible that for these fluids strain becomes localised in mid-plane, leading to a higher temperature rise than estimated. Another quite strong possibility is that these linear polymeric fluids experience some scission of the polymer molecules as they pass through the EHD contact leading to reduced friction. By sampling fluid through a small hole, Walker et al. [38] showed that polymeric base fluids can break down to lower molecular weight in EHD contacts at considerably lower shear stresses than those present in this study. An early rule of thumb for linear hydrocarbon chain polymers is that polymer molecule scission will start to occur when shear stress $\times$ MWt^2 > 1×10^{14} [39]. This would suggest that polymers of molecular weight greater than 1000 might be expected to breakdown in an EHD contacts of pressure
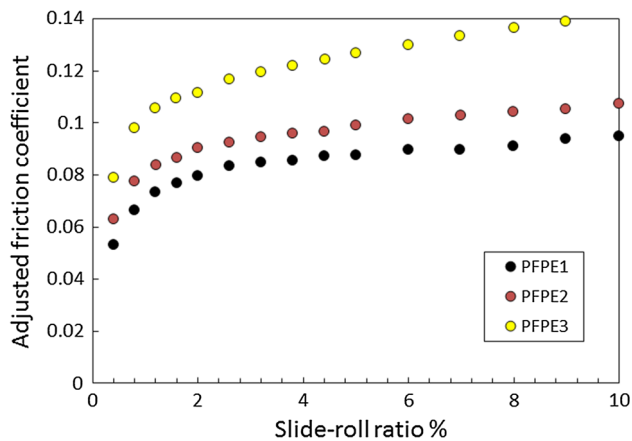
Fig. 11 Isothermally adjusted EHD friction coefficient versus slide–roll ratio for the PFPEs at mean pressure = 2 GPa, temperature = 60 °C
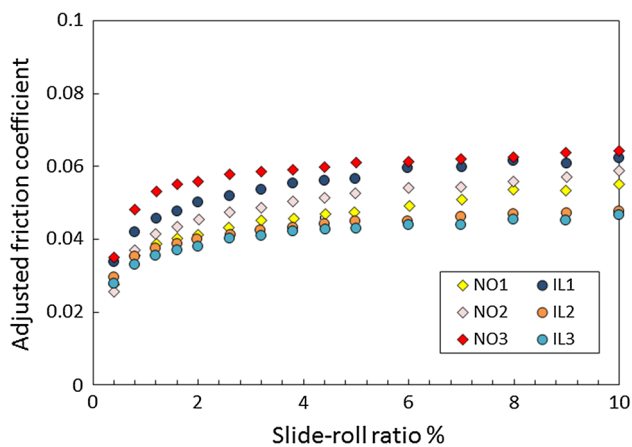

Fig. 12 Isothermally adjusted EHD friction coefficient versus low slide–roll ratio for the natural oils and ionic liquids at mean pressure = 2 GPa, temperature = 60 °C
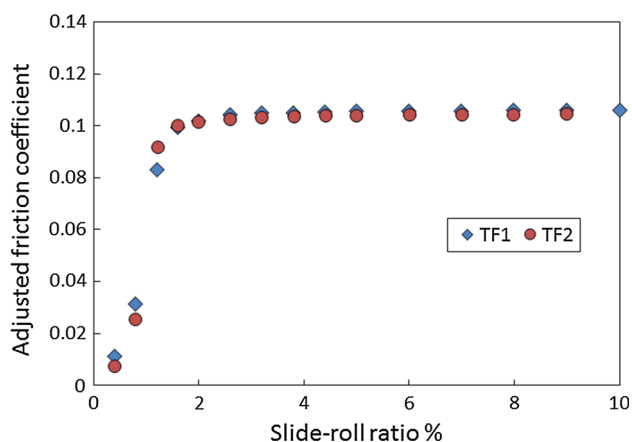

Fig. 13 Isothermally adjusted EHD friction coefficient at 5% SRR versus slide–roll ratio for the traction fluids at mean pressure = 2 GPa, temperature = 60 °C

2 GPa and friction coefficient of 0.05, although we do not know whether a significant scission would occur within the time of passage through the contact. If significant polymer base oil breakdown does occur in high pressure rolling/sliding EHD contacts, it is difficult to usefully interpret the EHD rheology of such fluids in such conditions.

A general problem in this type of analysis with all of the polymer-based fluids, PG1 to PG5 and PFPE1 to PFPE3, is that their relatively high viscosity leads to high film thickness, reaching several hundred nanometres. At the EHD thickness increases, the second term in Eq. 6, expressing how much hotter the oil film is than the surfaces, starts to dominate. Since this term is based on assumptions as to the thermal conductivity of the oil and the shape of the velocity gradient, this means that for viscous fluids the estimation of oil film temperature becomes less reliable.

The linear dependence of isothermally corrected friction coefficient on log(SRR) for most fluids implies, as indicated in Eqs. 4 and 5, that mean shear stress varies linearly with log(strain rate);

$$\tau = c_0 + c_1 \log_e \dot{\gamma} \tag{11}$$

It is thus possible generalise the calculated isothermal EHD friction data via the two constants c_0 and c_1 to enable calculation of EHD friction at other contact conditions. These constants (in MPa) are listed in Tables 4 and 5, together with the maximum strain rates up to which they can be used with confidence. These strain rates correspond to the conditions at which the 8 °C temperature rise limit was reached and thus depend on the friction coefficient and film thicknesses of the fluid concerned. Using these constants, it is possible to construct isothermal EHD friction curves for these fluids. Fluids PG1–PG5, PFPE1–PFPE3, TF1 and TF2 are not listed in Tables 4 and 5. The calculated isothermal mean shear stress values for the polymeric fluids are unreliable for reasons outlined above while TF1 and TF2 reach limiting shear stresses.

As discussed in [31] a logarithmic dependence of shear stress on strain rate is expected from the Eyring rheological model at the high shear stresses present above SRR = 1% in the high-pressure contacts studied. According to this model the constant c_1 in Eq. 11 should represent the Eyring stress, τ_e, while the constant c_0 should correspond to the value $\log_e(2\eta_p/\tau_e)$ where η_p represents the low shear rate viscosity within the contact. It should be noted, however, that the most appropriate rheological model to describe the relationship between fluid stress and strain in high pressure EHD contacts is still a topic of considerable debate [31, 40, 41] and the fit values in Tables 4 and 5 are provided to enable readers to construct isothermal EHD friction curves and not to espouse any particular model of EHD rheology.

Table 4 Fit constants of $\bar{\tau} = c_0 + c_1 \ln \dot{\gamma}$ at mean contact pressure of 1.5 GPa

Fluid	$p_{mean} = 1.5$ GPa								
	60 °C			80 °C			100 °C		
	c_0 (MPa)	c_1 (MPa)	$\dot{\gamma}_{max} \times 10^6$	c_0 (MPa)	c_1 (MPa)	$\dot{\gamma}_{max} \times 10^6$	c_0 (MPa)	c_1 (MPa)	$\dot{\gamma}_{max} \times 10^6$
E1	−86.2	13.3	3	−105.6	13.4	5	−132.0	14.1	10
E2	−124.4	14.0	6	−152.9	14.6	8	−170.8	14.8	13
E3	−63.0	10.6	3	−86.3	11.3	6	−111.2	11.9	12
E4	−171.1	16.3	11	−187.8	16.2	16	−189.2	15.4	20
E5	−164.2	16.0	7	−190.9	16.6	12	−199.1	16.0	17
E6	−160.0	15.6	8	−195.9	16.6	13	−196.5	15.5	21
E7	−99.7	13.2	4	−140.6	14.5	8	−166.2	15.0	11
E8	−124.6	13.1	4	−159.8	14.2	9	−162.8	13.4	13
E9	−63.0	10.5	3	−113.3	12.9	5	−147.6	14.1	7
E10	−122.8	13.2	5	−160.1	14.8	7	−185.6	15.3	13
PG6	−86.4	12.8	3	−138.8	15.0	5	−159.8	15.0	8
PG7	−133.3	14.4	6	−159.0	14.8	11	−178.7	15.1	16
PAO1	−176.0	16.2	12	−184.2	15.6	17	−194.1	15.3	21
PAO2	−133.0	14.8	4	−162.8	15.5	6	−181.1	15.7	10
PAO3	−117.6	14.0	3	−148.4	14.9	5	−164.0	14.9	8
PAO4	−87.2	12.8	1.5	−134.7	15.1	2	−141.8	14.2	4
MO1	−67.2	12.0	2	−100.0	13.1	4	−122.3	13.6	6
MO2	−54.6	11.0	2	−91.5	12.5	4	−122.1	13.6	8
MO3	−90.5	12.3	5	−126.1	13.5	8	−156.2	14.4	12
MO4	−82.4	12.8	2	−115.1	13.9	4	−136.7	14.2	6
MO5	−70.2	12.0	1.5	−115.4	13.9	3	−136.3	14.2	6
PIB	24.0	7.9	1	16.2	7.7	3	−22.5	9.7	4
NO1	−123.6	12.7	5	−140.6	12.5	9			
NO2	−105.2	11.7	4	−138.4	12.8	7	−144.7	12.3	11
NO3	−2.8	5.6	1.5	−82.7	10.2	3	−120.8	11.6	6
IL1	−78.3	11.6	0.6	−122.7	13.5	2	−144.9	13.8	4
IL2	−61.8	8.2	7	−95.1	9.5	10	−124.6	10.6	16
IL3	−70.8	9.0	4	−102.8	10.2	8	−124.7	10.8	12

c_0, c_1 only valid up to the value $\dot{\gamma}_{max}$ listed

7 Conclusions

This paper has compared the EHD friction properties of a wide range of generally well-defined base fluids at three temperatures and two pressures. The use of tungsten carbide ball and disc specimens enabled high contact pressures, comparable to those present in rolling bearings, to be reached.

The study confirms previous work in showing the importance of molecular structure of the base fluid in determining EHD friction. Liquids having linear-shaped molecules with flexible bonds give considerably lower friction that liquids based on molecules with bulky side groups or rings. EHD friction also increases with viscosity for liquids having similar molecular structures. Using pure ester fluids, it is shown that quite small differences in molecular structure can have considerable effects on EHD friction.

The importance of temperature rise in reducing EHD friction at slide–roll ratios above about 5% is demonstrated. By measuring EHD friction at several temperatures and pressures, and also measuring EHD film thickness in order to estimate strain rates of the EHD films, it is possible to make approximate corrections to measured EHD friction data in order to obtain isothermal EHD friction curves. In principle, these can be used, in

Table 5 Fit constants of $\bar{\tau} = c_0 + c_1 \ln \dot{\gamma}$ at mean contact pressure 2.0 GPa

Fluid	$p_{mean} = 2.0$ GPa								
	60 °C			80 °C			100 °C		
	c_0 (MPa)	c_1 (MPa)	$\dot{\gamma}_{max} \times 10^6$	c_0 (MPa)	c_1 (MPa)	$\dot{\gamma}_{max} \times 10^6$	c_0 (MPa)	c_1 (MPa)	$\dot{\gamma}_{max} \times 10^6$
E1	−70.5	15.7	2	−99.7	16.4	3	−126.2	17.0	5
E2	−133.8	18.0	2	−151.3	17.7	6	−181.4	18.4	8
E3	−53.7	13.3	2	−82.1	14.1	3	−120.6	15.4	7
E4	−156.6	19.0	5	−177.5	18.9	10	−206.8	19.6	10
E5	−151.5	18.8	4	−178.5	19.0	7	−214.6	20.0	9
E6	−138.1	17.6	4	−189.6	19.5	8	−227.0	20.4	13
E7	−125.3	19.1	3	−138.4	18.1	4	−158.6	17.9	7
E8	−145.0	18.4	2	−181.1	19.0	4	−191.5	18.2	7
E9	−72.9	15.4	1.5	−130.2	17.8	2	−156.2	18.0	4
E10	−141.1	18.0	3	−187.8	20.1	4	−225.5	20.9	9
PG6	−82.3	16.7	2	−122.6	17.7	3	−169.6	19.3	6
PG7	−150.0	19.5	3	−150.3	17.6	6	−197.5	19.4	8
PAO1	−165.0	18.8	8	−204.0	19.9	10	−212.6	19.2	13
PAO2	−140.2	19.1	1	−177.1	19.9	4	−200.5	20.1	6
PAO3	−125.7	18.5	1.5	−156.9	18.9	4	−176.9	19.0	5
PAO4	−78.7	16.2	'	−128.9	18.2	1.5	−158.0	18.6	3
MO1	−51.5	14.8	1.5	−89.0	16.0	3	−129.4	17.5	4
MO2	−73.6	16.4	1.5	−97.3	16.6	3	−130.7	17.6	4
MO3	−94.8	16.4	3	−120.4	16.5	4	−155.8	17.6	7
MO4	−64.8	15.5	1.5	−95.0	16.2	2	−153.7	18.8	3
MO5	−65.9	15.9	1	−113.1	17.5	2	−135.8	17.6	3
PIB	−32.0	15.6	1	15.7	11.4	2	−11.3	12.5	3
NO1	−139.2	17.3	2.5	−163.9	17.1	5			
NO2	−113.0	16.0	2.5	−155.8	17.2	3	−171.2	16.8	5
NO3	13.0	8.5	0.7	−84.3	13.9	2	−135.3	15.7	3
IL1	−77.4	15.5	0.5	−131.5	17.7	1	−174.6	19.0	2
IL2	−38.9	9.1	3	−75.9	10.7	6	−122.5	12.9	9
IL3	−48.5	9.8	3	−94.0	11.9	5	−119.6	12.7	7

c_0, c_1 only valid up to the value $\dot{\gamma}_{max}$ listed

conjunction with calculated temperature rises, to estimate EHD friction coefficients in other contact geometries and conditions.

Appendix 1: Base Fluid Structures

Esters

E1 and E2 are both dibasic acid esters of phthalic acid having the chemical structure shown below.
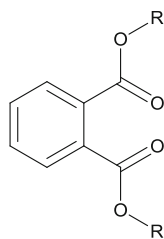
Molecular structure of E1 and E2

E1 has ethylhexyl-R groups while those in E2 are *n*-octyl-.

R =

ethylhexyl-

R =

n-octyl
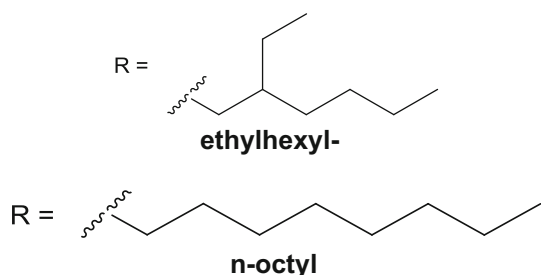
E3–E6 are all esters formed by the reaction of a dibasic acid with 2-ethylhexanol, so R is always ethylhexyl-.

E3 is the diester of teraphthalic acid with the structure shown below. Thus it differs from E1 only in the relative positions of the ester groups on the benzene ring.
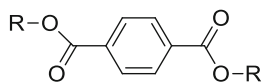
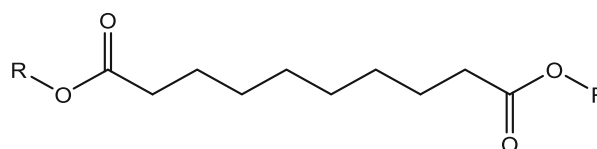**Molecular structure of oil E3, (diethylhexyl teraphthalate)**

E4–E6 are dibasic acid esters differing only in the length of the dibasic acid chain, as shown below.
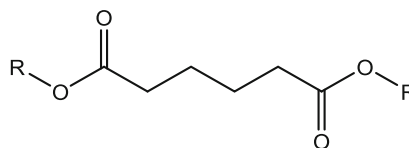
Molecular structure of E4, (diethylhexyl adipate)
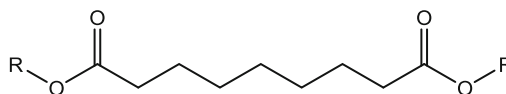
Molecular structure of E5, (diethylhexyl azelate)

Molecular structure of E6, (diethylhexyl sebacate)

E7 is diisododecylazelate with the structure shown below.
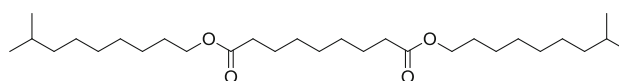
Molecular structure of E7, (diisodecyl azelate)

Oils E8 and E9 are polyol esters based on neopentyl glycol which has two esterifiable OH groups. E8 is an oleate ester while E9 is a diisostearate ester.
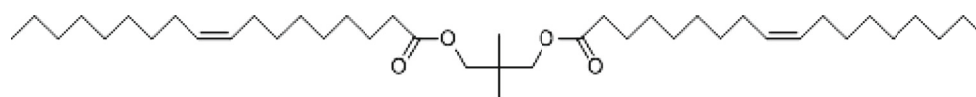
Molecular structure of E8, (NPG Dioleate)
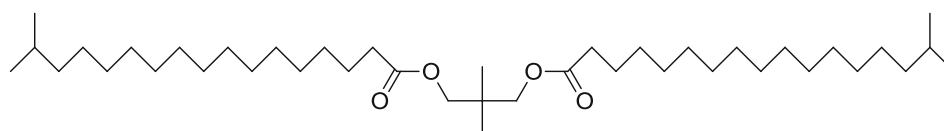
Molecular structure of E9, (NPG Diisostearate)

E10 is a polyol esters based on trimethylol propane having three esterifiable OH groups and having the structure shown below. The R groups are mixed alkyls have between 8 and 10 carbon atoms.
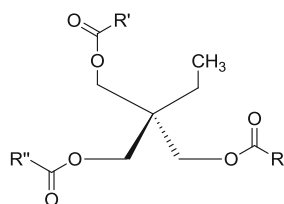
Molecular structure of E10

Polyalkylene Glycols

The polyalkylene glycols (PAGs) are polyethers of ethylene oxide (EO) and propylene oxide (PO) formed from a nucleophilic initiator such as an alcohol. Generally PAGs formed with a large proportion of EO are water soluble, whereas PAGs formed with a PO are oil soluble. EO/PO copolymers have limited water solubility dependent on the EO/PO ratio.

PG1 and PG2 both contain EO and PO, randomly arranged. Both are based on a triol, PG1 on trimethylpropane, with the A, A′, A″ alkoxy groups having a ratio of 3 EO to 1 PO, and PG2 on glycerol with the alkoxylate chains having a ratio 1 EO to 1 PO. They have the structures shown below.
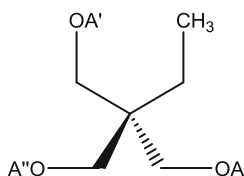
Molecular structure of PG1, (TMP 3:1 EO:PO)
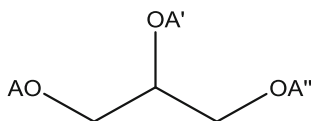
Molecular structure of PG2, (Glycerol 1:1 EO:PO)
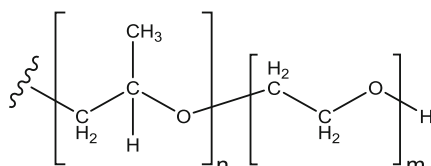
A, A', A'' groups for EO:PO PAGs

PG3–PG5 contain only the PO repeating unit (propoxylate), and all take the form shown below. In PG3 and PG4, the R group is a four carbon chain (butyl) but n is larger in PG4. In PG5, the alkyl R group is a 12–14 carbon alkyl chain.
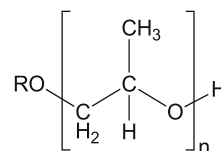
Molecular structure of PG3 to PG5

PG6 and 7 are both polyethers with a similar structure to that of PG3–PG5 above but with short propoxylate chains In PG6, the R group is a 16 carbon alkyl chain and $n = 10$ while PG7 has a 14 carbon alkyl chain R group and $n = 3$.

Polyalphaolefins

Oils PAO1–PAO4 are conventional polyalphaolefins (PAOs) of varying viscosities. These are all based on hydrogenated oligomers of n-dec-1-ene with between 2 and 6 monomer groups.

Mineral Oils

MO1–MO5 are all mineral oils. MO1 is Group I, MO2 group II and MO3 to MO5 are group III.

Traction Fluids

TF1 is a high traction base fluid, 2,4-dicyclohexyl-2-methylpentane, obtained from Santolubes LLC and having the chemical structure shown below.
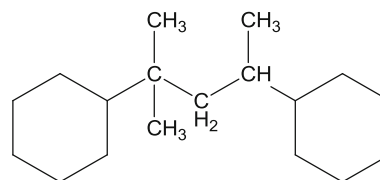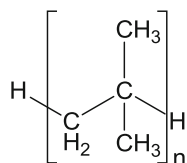

Molecular structure of TF1

TF2 is a high traction base fluid DM2H, 2,3-dimethyl-2-[(3-methylbicyclo[2.2.1]hept-2-yl)methyl]bicyclo[2.2.1]heptane, obtained from Idemitsu Kosan and having the structure shown below [42].
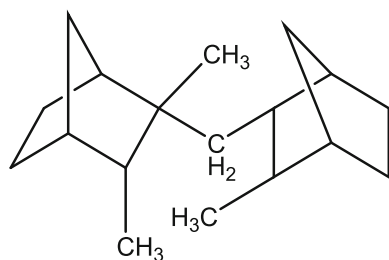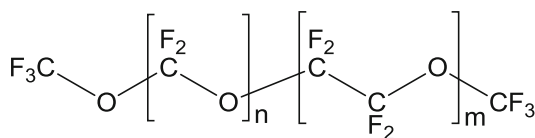
Molecular structure of TF2

Polyisobutylene

Polyisobutylene (PIB) has the chemical structure shown below. For the fluid tested n is predominantly in the range 4–7.

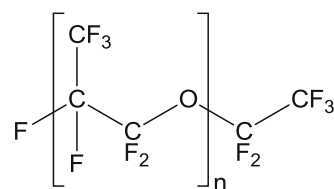**Molecular structure of PIB**

Perfluoropolyethers

PFPE1 and PFPE2 are both Z-type PFPEs with chemical structure shown below. They differ in the lengths of their chains and the ratio of n to m.

**Molecular structure of PFPE1 and PFPE2**

PFPE3 is a K-type PFPE. Unlike PFPE1 and PFPE2 this fluid has CF_3 side groups.

Molecular structure of PFPE3

Natural Oils

Oil NO1–NO3 are natural (biobased) oils extracted from plants. They are all esters of glycerol having predominant chemical structure of the form shown below where the R, R′ and R″ alkyl and alkenyl groups are the carbon chains of the fatty acids prior to esterification.
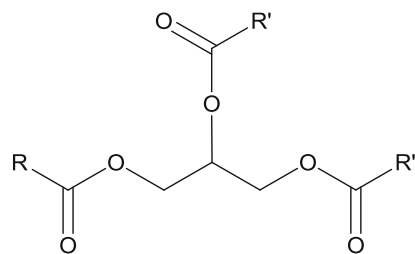
Molecular structure of triglyceride natural oils

Oils NO1–NO3 are characterised by the fatty acid compositions shown in Table 6. The fatty acids can be classified by their number of carbon atoms and their degree of saturation, represented by the number of double bonds they contain.
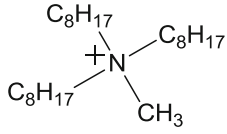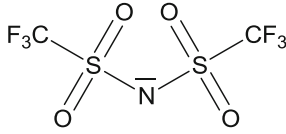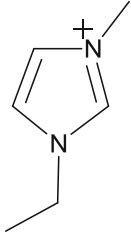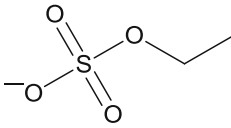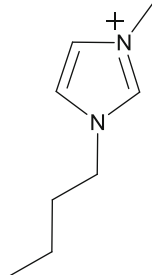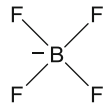
Ionic Liquids

Oils IL1–IL3 are room-temperature ionic liquids. The molecular structures of their ions are shown in Table 7 below.

Table 6 Compositions of main fatty acids in oils NO1–3

Name	No. of C atoms	No. of double bonds	No. of OH groups	Percentage fatty acid		
				NO1	NO2	NO3
Palmitic	16	0	0	3.84	11.28	2.63
Stearic	18	0	0	4.42	2.7	1.51
Oleic	18	1	0	83.66	24.39	4.74
Linoleic	18	2	0	8.08	56.28	8.36
Linolenic	18	3	0	Trace	5.34	Trace
Ricinoleic	18	1	1	–	–	82.8

Table 7 Structures of ionic liquids studied

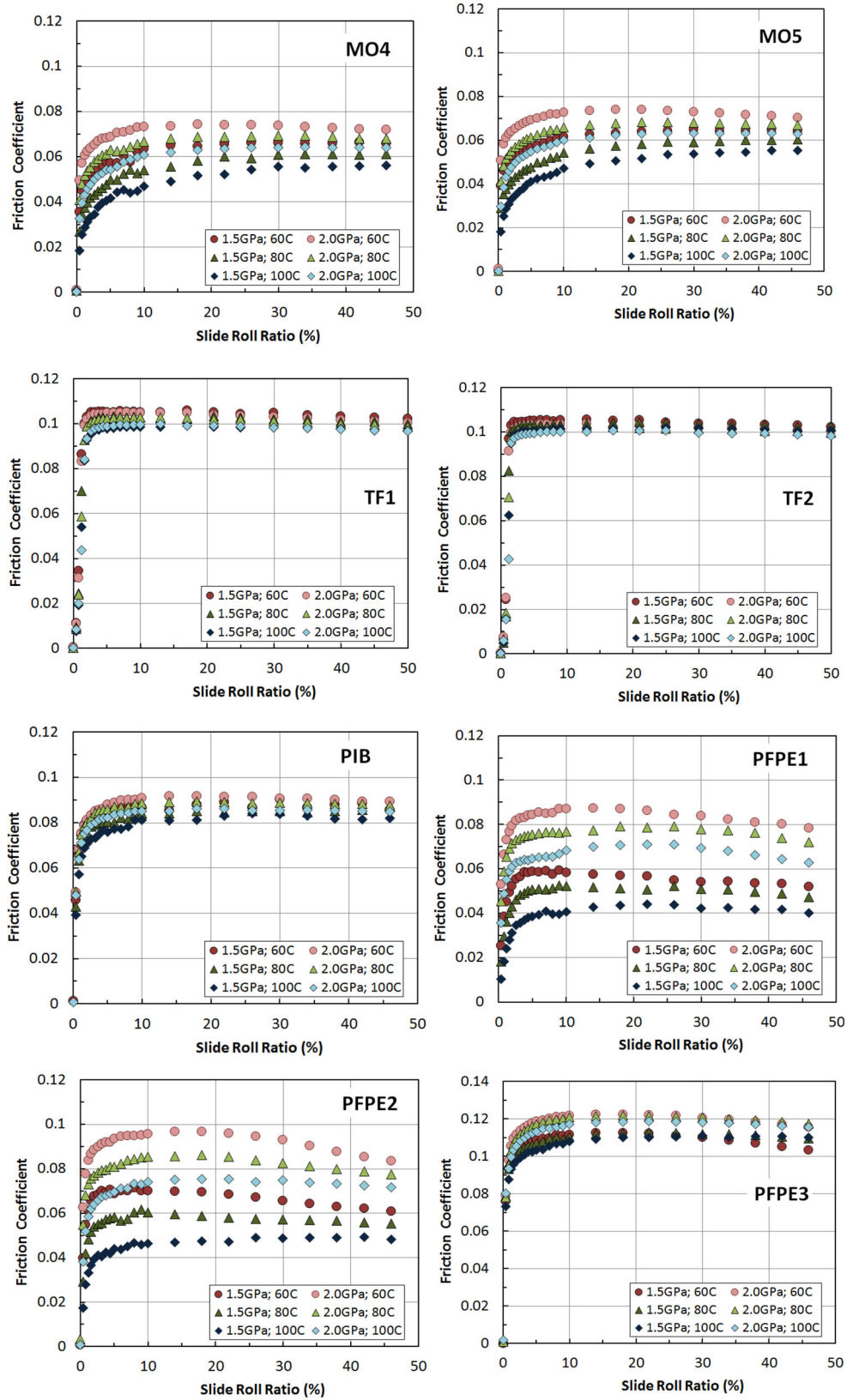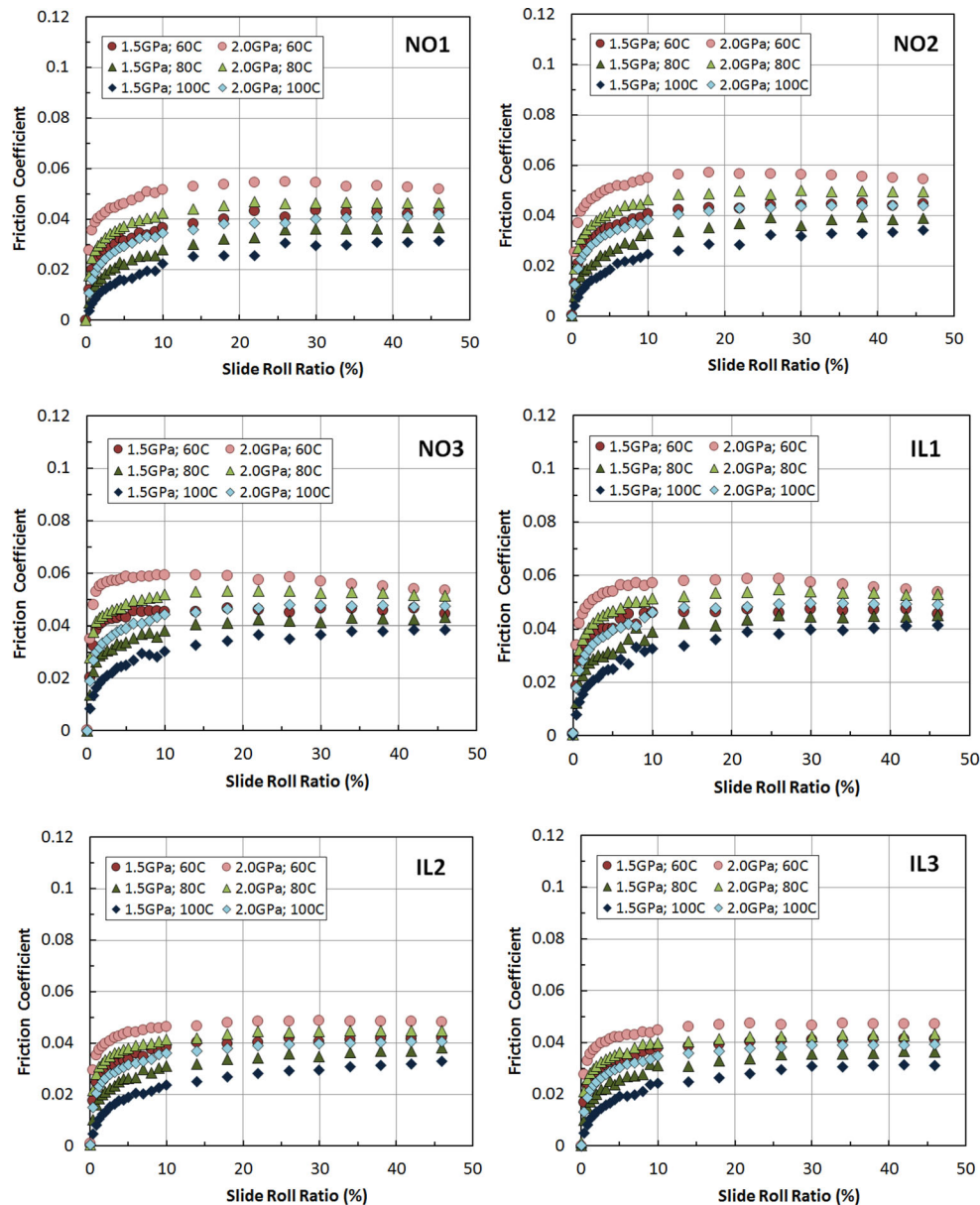|	cation	anion
IL1	Methyl-trioctylammonium	Bis(trifluoromethylsulfonyl) imide
IL2	1-Ethyl-3-methylimidazolium	Ethyl sulfate
IL3	1-Butyl-3-methylimidazolium	Tetrafluoroborate

Appendix 2: EHD Friction Data

Note that fluid PFPE3 has a different friction coefficient scale from the other graphs.
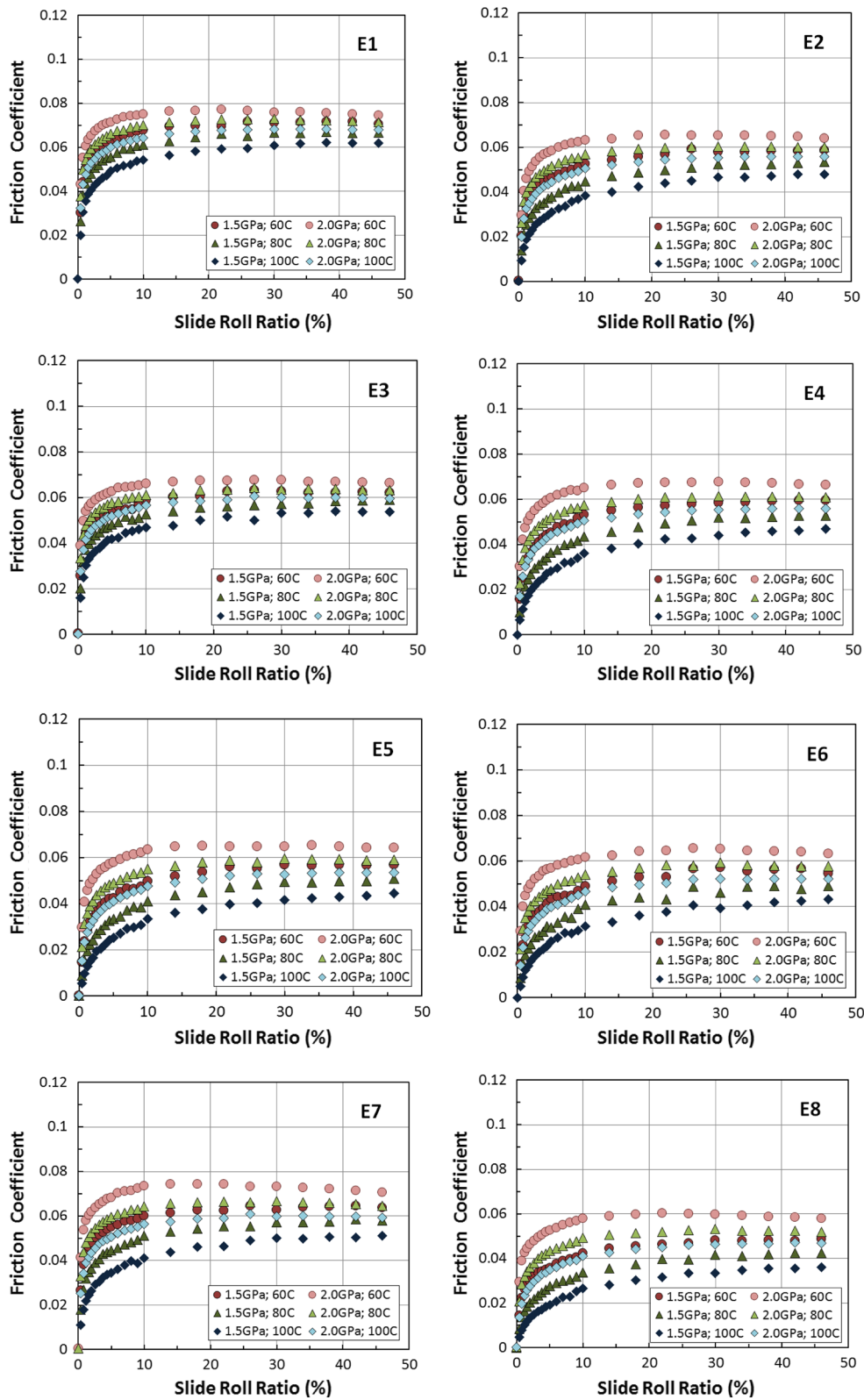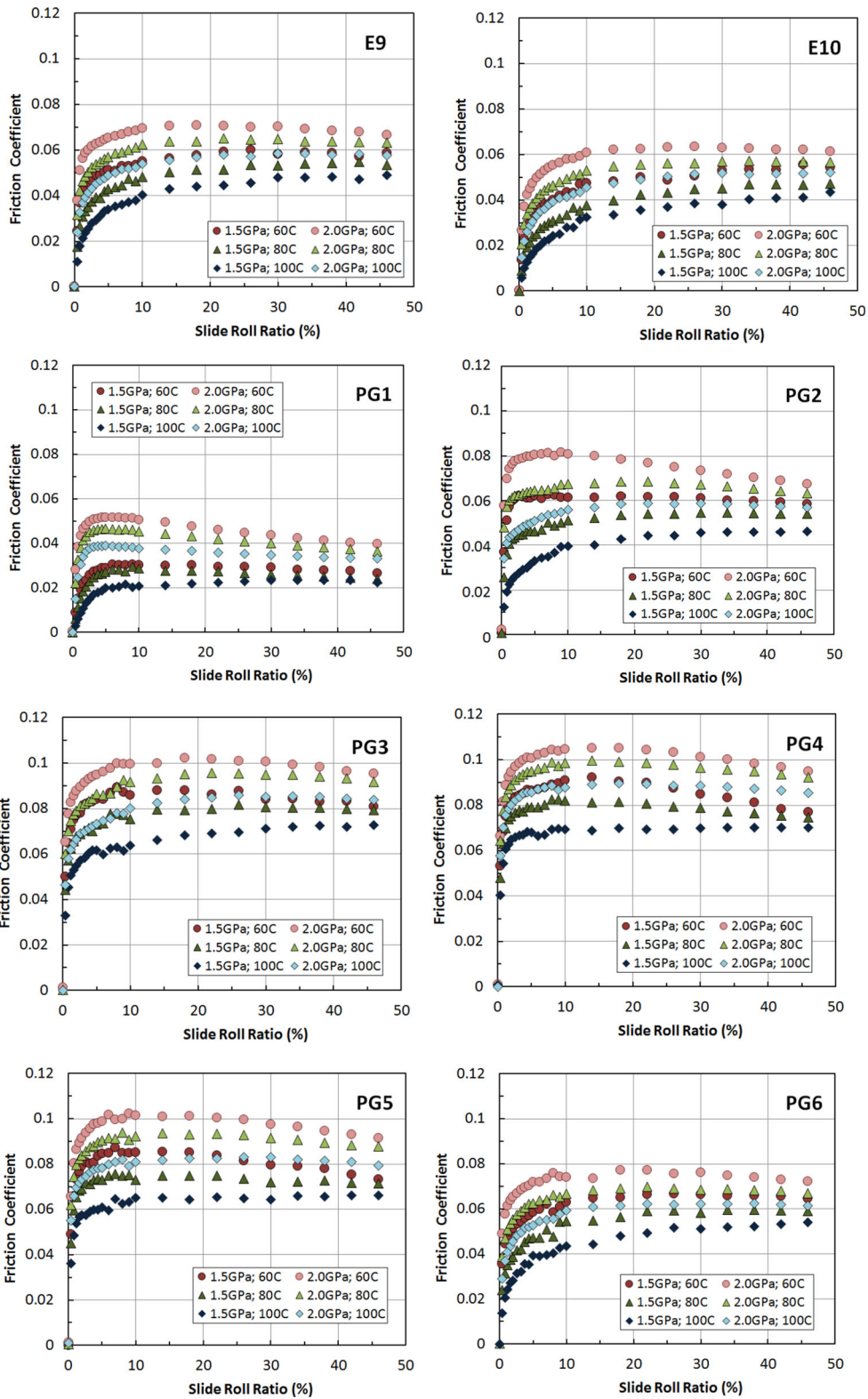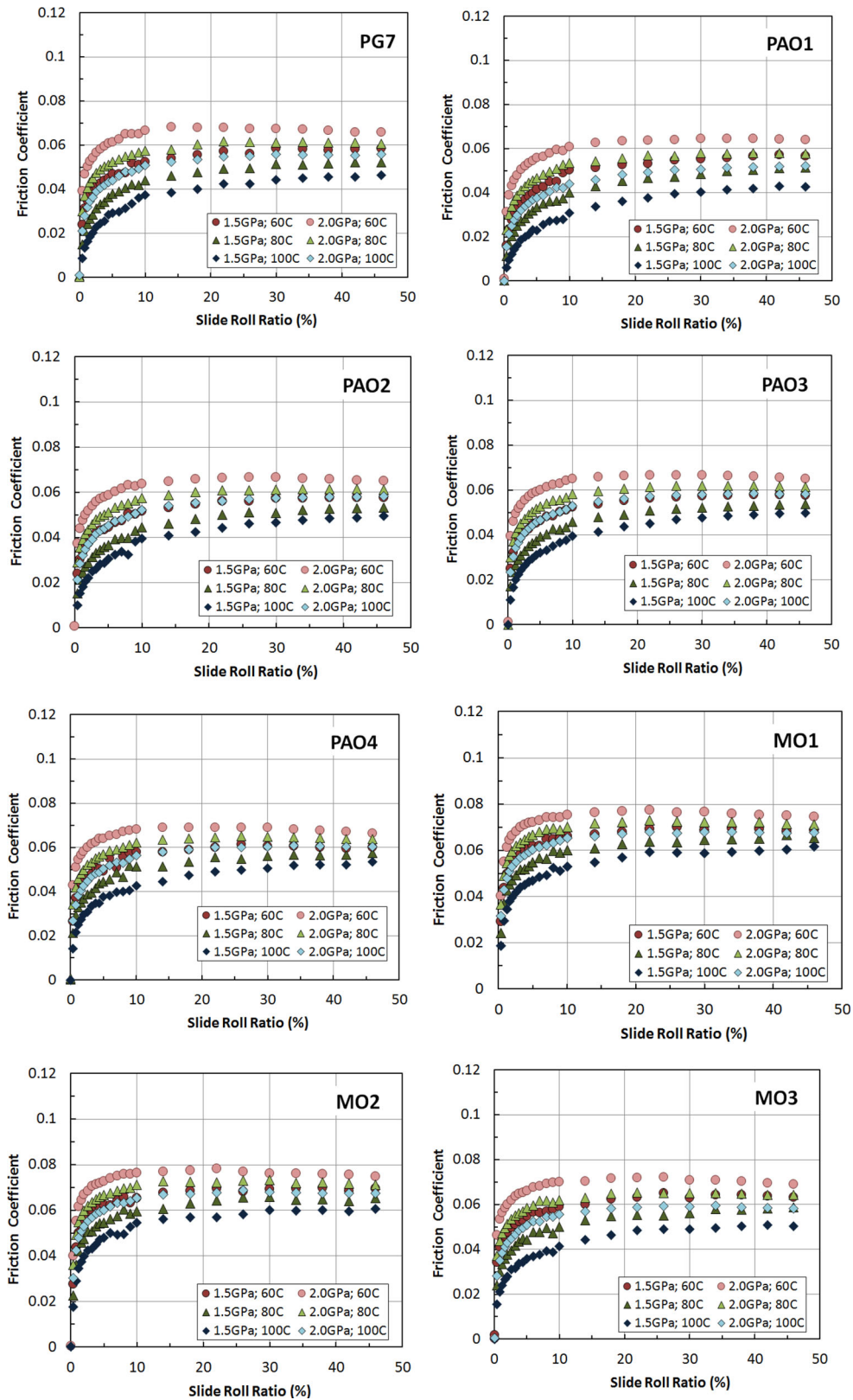
References

1. Rounds, F.G.: Effects of lubricant composition on friction as measured with thrust ball bearings. J. Chem. Eng. Data **5**, 499–507 (1960)
2. Cecil, R., Pike, W.C., Raje, N.R.: Development of methods for evaluating traction fluids. Wear **26**, 335–353 (1973)
3. Smeeth, M., Gunsel, S., Korcek, S.G., Spikes, H.A.: The elasto-hydrodynamic friction and film-forming properties of lubricant base oils. Tribol. Trans. **42**, 559–569 (1999)
4. Hammann, W.C., Schisla, R.M., Groenweghe, L.C.D., Gash, V.W.: Synthetic fluids for high capacity traction drives. ASLE Trans. **13**, 105–116 (1970)
5. Hentschel, K.-H.: The influence of molecular structure on the frictional behaviour of lubricating fluids. J. Synth. Lubr. **2**, 143–174 (1985)
6. Muraki, M.: Molecular structure of synthetic hydrocarbon oils and their rheological properties governing traction characteristics. Tribol. Int. **20**, 347–354 (1987)
7. Toshiyuki, T., Hitoshi, H.: The fundamental molecular structures of synthetic traction fluids. Tribol. Int. **27**, 183–187 (1994)
8. Tsubouchi, T., Hata, H.: Study on the fundamental molecular structures of synthetic traction fluids: part 2. Tribol. Int. **28**, 335–340 (1995)
9. Hata, H., Tsubouchi, T.: Molecular structures of traction fluids in relation to traction properties. Tribol. Lett. **5**, 69–74 (1998)
10. Tsubouchi, T., Hata, H., Yoshida, Y.: Optimisation of molecular structure for traction fluids. Lubr. Sci. **16**, 393–403 (2004)
11. Chapaton, T.J., Capehart, T.W., Linden, J.L.: Synthesis and characterization of alkyl-bridged bicycloheptanes as traction fluids. Tribol. Trans. **49**, 454–472 (2006)
12. Zolper, T., Li, Z., Jungk, M., Stammer, A., Stoegbauer, H., Marks, T., Chung, Y.-W., Wang, Q.: Traction characteristics of siloxanes with aryl and cyclohexyl branches. Tribol. Lett. **49**, 301–311 (2013)
13. Edgar, J.A., Hurley, S.: The use of quantitative structure activity relationships (QSAR) in traction fluid design. SAE Technical Paper 37, 2004-01-2009 (2004)

14. Hirst, W., Moore, A.J.: Elastohydrodynamic lubrication at high pressures. II. Non-Newtonian behaviour. Proc. R. Soc. A **365**, 537–565 (1979)
15. Hentschel, K.-H.: The influence of molecular structure on the frictional behaviour of lubricating fluids 2: low coefficients of traction. J. Synth. Lubr. **2**, 238–260 (1985)
16. Chang, H.-S., Bunemann, T., Spikes, H.A.: The shear stress properties of ester lubricants in elastohydrodynamic contacts. J. Synth. Lubr. **9**, 91–114 (1992)
17. LaFountain, A.R., Johnston, G.J., Spikes, H.A.: The elastohydrodynamic traction of synthetic base oil blends. Tribol. Trans. **44**, 648–656 (2001)
18. Yoshizaki, M., Naruse, C., Nemoto, R., Haizuka, S.: Study on frictional loss of spur gears (concerning the influence of tooth form, load, tooth surface roughness, and lubricating oil). Tribol. Trans. **34**, 138–146 (1991)
19. Höhn, B.R., Michaelis, K., Doleschel, A.: Frictional behaviour of synthetic gear lubricants. Tribol. Ser. **39**, 759–768 (2001)
20. Martins, R., Seabra, J., Brito, A., Seyfert, C., Luther, R., Igartua, A.: Friction coefficient in FZG gears lubricated with industrial gear oils: biodegradable ester vs. mineral oil. Tribol. Int. **39**, 512–521 (2006)
21. Michaelis, K., Höhn, B.R., Hinterstoißer, M.: Influence factors on gearbox power loss. Ind. Lubr. Tribol. **63**, 46–55 (2011)
22. Fernandes, C.M., Martins, R.C., Seabra, J.H.: Friction torque of cylindrical roller thrust bearings lubricated with wind turbine gear oils. Tribol. Int. **59**, 121–128 (2013)
23. Gentle, C.R., Cameron, A.: An investigation of traction in elastohydrodynamic point contacts using optical interferometry. ASLE Trans. **18**, 222–228 (1975)
24. Kyotani, T., Yoshitake, H., Ito, T., Tamai, Y.: Correlation between flow properties and traction of lubricating oils. ASLE Trans. **29**, 102–106 (1989)
25. ASME: Pressure-Viscosity Report. Viscosity and Density of Over 40 Lubricating Fluids of Known Composition at Pressure to 150,000 psi and Temperatures to 425F. ASME, New York (1953)
26. So, B.Y.C., Klaus, E.E.: Viscosity-pressure correlation of liquids. ASLE Trans. **23**, 409–421 (1980)
27. Spikes, H.A.: Thermodynamic approach to viscosity. Tribol. Trans. **33**, 140–148 (1990)
28. Johnston, G.J., Wayte, R., Spikes, H.A.: The measurement and study of very thin lubricant films in concentrated contacts. Tribol. Trans. **34**, 187–194 (1991)
29. Chittenden, R.J., Dowson, D., Dunn, J.F., Taylor, C.M.: A theoretical analysis of the isothermal elastohydrodynamic lubrication of concentrated contacts. I. Direction of lubricant entrainment coincident with the major axis of the Hertzian contact ellipse. Proc. R. Soc. Lond. Ser. A **397**, 245–269 (1985)
30. Biresaw, G., Bantchev, G.B.: Elastohydrodynamic (EHD) traction properties of seed oils. Tribol. Trans. **53**, 573–583 (2010)
31. Spikes, H.A., Zhang, J.: History, origins and prediction of elastohydrodynamic friction. Tribol. Lett. **56**, 1–25 (2014)
32. Archard, J.F.: The temperature of rubbing surfaces. Wear **2**, 438–455 (1959)
33. Larsson, R., Andersson, O.: Lubricant thermal conductivity and heat capacity under high pressure. Proc. Inst. Mech. Eng. J **214**, 337–342 (2000)
34. Ponjavic, A., Mare, L., Wong, J.S.: Effect of pressure on the flow behavior of polybutene. J. Polym. Sci. Part B Polym. Phys. **52**, 708–715 (2014)
35. Booser, E.R. (ed.): CRC Handbook of Lubrication and Tribology Volume III, Synthetic Lubricants. CRC Press, Boca Raton (1994)
36. Albert, J., Müller, K.: Thermal conductivity of ionic liquids: an estimation approach. Chem. Eng. Sci. **119**, 109–113 (2014)
37. Evans, C.R., Johnson, K.L.: The rheological properties of elastohydrodynamic lubricants. Proc. Inst. Mech. Eng. C **200**, 303–312 (1986)
38. Walker, D.L., Sanborn, D.M., Winer, W.O.: Molecular degradation of lubricants in sliding elastohydrodynamic contacts. J. Lubr. Technol. **97**, 390–395 (1975)
39. Mackenzie, K., Jemmett, A.E.: Polymer shear stability. Wear **17**, 389–398 (1971)
40. Bair, S., Vergne, P., Kumar, P., Poll, G., Krupka, I., Hartl, M., Habchi, W., Larsson, R.: Comment on "History, origins and prediction of elastohydrodynamic friction" by Spikes and Jie in Tribology Letters. Tribol. Lett. **58**, 1–8 (2015)
41. Spikes, H.A., Zhang, J.: Reply to the Comment by Scott Bair, Philippe Vergne, Punit Kumar, Gerhard Poll, Ivan Krupka, Martin Hartl, Wassim Habchi, Roland Larson on "History, origins and prediction of elastohydrodynamic friction" by Spikes and Jie in Tribology Letters. Tribol. Lett. **58**, 17 (2015)
42. Goda, T.: The latest trend in traction fluids. Idemitsu Tribo review, No. 34, 21, 11–14 (2011)